

Post Cyclic Behaviour of Singapore Marine Clay

Le comportement post-cyclique de l'argile marine de Singapour

Ho J., Goh S.H., Lee F.H.
National University of Singapore

ABSTRACT: In this paper, the post-cyclic behaviour of remoulded Singapore Marine Clay is examined. Cyclic triaxial tests, followed by monotonic loading to failure, were performed on normally consolidated specimens (38mm diameter by 76mm height) within a cyclic strain range of approximately 0.7% to 1.4%. Results herein reveal that the effective stress paths under post-cyclic monotonic loading may take on different forms depending on the mean effective stress state of the specimen at the end of the cyclic loading phase. By normalizing the mean effective stress (p') against the effective consolidation pressure (p_c') of the specimen, the effective stress paths during the post-cyclic monotonic loading may be approximately grouped into three different regimes, according to the normalized mean stress (p'/p_c'). Within each normalized mean stress regime, the monotonic soil response is independent of the effective consolidation pressure, the cyclic strain amplitude and number of cycles applied during cyclic loading. The results suggest that the normalized mean stress after cyclic loading may be an important parameter in determining the subsequent stress path under undrained monotonic loading to failure.

RÉSUMÉ : Dans ce papier, le comportement post-cyclique de l'argile marine remaniée de Singapour est étudié. Des essais triaxiaux cycliques suivis de chargement monotone jusqu'à la rupture ont été effectués pour des déformations cycliques comprises entre 0,7% et 1,4% sur des échantillons normalement consolidés. Les résultats démontrent que les chemins de contrainte durant le chargement monotone post-cyclique peuvent être de formes différentes et dépendent de l'état de contrainte moyenne effective de l'échantillon à la fin de la phase du chargement cyclique. En normalisant la contrainte moyenne effective (p') par la contrainte de consolidation (p_c'), les chemins de contrainte pendant le chargement monotone post-cyclique peuvent être regroupés en trois différents groupes selon la contrainte moyenne normalisée (p'/p_c'). Dans tous les cas, la réponse monotone du sol est indépendante de la contrainte effective de consolidation, de l'amplitude de la déformation cyclique et du nombre de cycles appliqué pendant le chargement cyclique. Les résultats suggèrent que la contrainte moyenne normalisée après le chargement cyclique pourrait être un paramètre important pour déterminer, sous chargement monotone non-drainé, les chemins de contrainte jusqu'à la rupture.

KEYWORDS: Post-cyclic clay behaviour, Mean effective stress, Cyclic stress reversal

1 INTRODUCTION

Previous studies have shown that, during undrained compression loading, the effective stress path of a normally consolidated clay after cyclic loading is similar to the effective stress path of an overconsolidated clay (Hyde and Ward 1985, Matsui et al. 1992, Yasuhara et al. 1992). Researchers have adopted different frameworks in the analysis of the post-cyclic undrained shear strength of clays. One common approach is to estimate the undrained shear strength based on the maximum shear strain during the applied cyclic loading (Thiers and Seed 1969, Sangrey and France 1980). Another method of analysis is to relate the post-cyclic undrained shear strength with the apparent overconsolidation ratio induced by the cyclic loading (Matsui et al. 1992, Yasuhara et al. 1992). Apart from the post-cyclic undrained shear strength, this induced apparent overconsolidation ratio from cyclic loading was also used to determine how the subsequent monotonic effective stress path approaches the critical state line (Yasuhara et al. 1992).

However, one possible limitation in past studies is the relatively fast rates of cyclic loading used, which typically ranges from 0.5Hz to 1 Hz. At such loading rates, it is uncertain if excess pore pressure in the clay specimens will be able to dissipate. For this reason, the reliability of pore pressure measurements during cyclic loading phase may be doubtful. Fast loading rates on normally consolidated clays during undrained triaxial tests prevents equilibration of excess pore pressure within test specimens, which results in a higher pore pressure within the middle one-third portion of the specimen

(Wood 1982). This can lead to errors in effective stress calculations. Few attempts had been made to overcome the issue of unequalized pore pressures during cyclic loading. For example, Matsui et al (1992) the specimen to stand in an undrained state for 1 hour after cyclic loading and prior to post-cyclic monotonic loading to allow for equalization of pore pressures. On the other hand, Diaz-Rodriguez et al (2000) used a longer equalization period of 12 hours. Another approach is to allow drainage before post-cyclic loading to allow for pore pressures accumulated during cyclic loading to be dissipated (Yasuhara et al. 1992). The drawback of this approach is that it alters the pore pressures within specimens, leading to discontinuities in effective stress paths between the cyclic loading and post-cyclic loading phases. Intuitively, the effective stress response of a clay undergoing cyclic loading should be indicative of its post-cyclic behavior if post-cyclic monotonic loading is conducted immediately after cyclic loading. Due to possible errors effective stress measurements and discontinuities between cyclic and post-cyclic effective stress paths, a direct comparison between the cyclic and post-cyclic behavior of clays has hitherto not been possible. This objective of the study reported herein is to re-visit the issue of post-cyclic behaviour of soft clay, while ensuring adequate equilibration of excess pore pressure.

2 CYCLIC AND POST CYCLIC TESTING PROGRAM

A series of two way strain-controlled undrained cyclic triaxial tests were performed on remoulded specimens (38mm diameter by 76mm height) of normally consolidated Singapore Upper

Marine Clay, the standard properties of which have been reported by Tan (1983). After cyclic loading, the specimens were immediately subjected to standard consolidated undrained triaxial monotonic loading to failure. According to Ho et al. (2012), when undrained cyclic triaxial tests on clays are conducted at a sufficiently slow rate for pore pressure equilibration, intrinsic strain rate effects on pore pressure measurements, effective stress paths and stress-strain relationships are negligible. Since the focus of this study is not on strain rate effects, all tests were conducted at relatively slow rates. Both mid-plane and base pore pressure transducers were used and pore pressure equilibration is considered to be achieved when both transducers produce similar excess pore pressure measurements. All cyclic and post-cyclic triaxial tests were performed using the GDS Enterprise Level Dynamic Triaxial Testing System. Table 1 shows the experimental matrix. Experimental data presented in this study was recorded at 2-second intervals.

Table 1. Experimental Matrix.

No	Effective Consolidation Pressure, p_c' (kPa)	Cyclic Amplitude		Period (min)	No. of Cycles
		Amplitude (mm)	Strain (%)		
1	50	-		-	0
2		-		-	5
3		-		-	10
4		1	≈ 1.4	10	15
5		1	≈ 1.4	10	20
6		1	≈ 1.4	10	100
7	100	-		-	0
8		-		-	2
9		-		-	3
10		-		-	4
11		1	≈ 1.4	14	5
12		1	≈ 1.4	14	6
13		1	≈ 1.4	14	20
14		1	≈ 1.4	14	30
15		1	≈ 1.4	14	100
16	200	-		-	0
17		-		-	2
18		-		-	3
19		-		-	4
20		1	≈ 1.4	60	5
21		1	≈ 1.4	60	6
22		1	≈ 1.4	60	10
23		1	≈ 1.4	60	30
24		1	≈ 1.4	60	100

3 EXPERIMENTAL RESULTS AND DISCUSSION

3.1 Cyclic Loading

Normalized stress plots and stress-strain relationships during the cyclic tests are summarized in Figure 1. The stress path parameters, i.e. deviator stress (q) and mean effective stress (p'), are normalized against the effective consolidation pressure (p_c') for easy comparison between specimens subjected to different consolidation pressures. Post-cyclic effective stress paths are included in Figure 1. The critical state line is also plotted based on data from monotonic triaxial compression tests where the effective angle of friction for Singapore Upper Marine Clay is found to be 25.4 degrees. The initial yield locus and the state boundary surface are assumed to be elliptical.

For Singapore Upper Marine Clay specimens subjected to the same effective confining pressure, the stress paths and stress-strain relationships shown on Figure 1 for different number of applied cycles are similar, reflecting consistency among the specimens. Due to positive excess pore water

pressure generated during cyclic loading, the mean effective stress generally decreases during the reloading phase of each cycle. However, after a certain number of load cycles, the mean effective stress is observed to increase at the later part of the loading, just before the maximum deviator stress is reached, as illustrated in Figure 2. The turning point marking this change in mean effective stress is hereby termed as "stress reversal" point. These stress reversal points correspond to a decrease in shear-induced excess pore water pressure, which would seem to imply dilative behavior. As the stress reversal points appear after the normalized mean effective stress decreases beyond a certain value, post-cyclic monotonic tests are conducted after different number of load cycles to investigate the factors governing the onset of this stress reversal behaviour.

3.2 Post-cyclic Loading

Normalized stress plots and stress-strain relationships during the post-cyclic monotonic tests are summarized in Figure 3, for the tests listed in Table 1. From Figure 3, the form of the effective stress paths under post-cyclic monotonic loading depends on the normalized mean effective stress state of the specimen at the start of the post-cyclic loading phase. These post-cyclic effective stress paths may be approximately grouped into three different regimes, according to the normalized mean effective stress.

When the normalized mean effective stress state of the clay specimen at the start of post-cyclic monotonic loading is greater than 0.6, stress reversal is generally absent and post-cyclic shearing shows either a decrease or no change in mean effective stress. This is akin to that of lightly over-consolidated and normally consolidated clays which tend to increase in density when sheared.

On the other hand, when the normalized mean effective stress state of the clay specimen at the start of post-cyclic monotonic loading falls below 0.5, stress reversal becomes evident and the effective stress path becomes similar to that of heavily over-consolidated clays.

Within the range of 0.5 to 0.6, the effective stress path is approximately vertical indicating that this is a boundary zone between occurrence or otherwise, of stress reversal.

Unlike the effective stress paths, the normalized stress-strain relationships are relatively similar. The post-cyclic undrained strength is almost equal to that without cyclic loading. This means that the undrained shear strength of Singapore Upper Marine Clay is not significantly influenced by cyclic loading. This observation agrees with the findings of Yasuhara et al. (1992).

3.3 Effect of Cyclic Strain Amplitude

In this section, the results of four additional tests conducted at a lower strain amplitude are presented; the aim being to investigate whether strain amplitude has any effect on the stress reversal. Table 2 summarizes the four additional tests conducted.

Table 2. Additional Cyclic and Post-cyclic Tests.

No	Effective Consolidation Pressure, p_c' (kPa)	Cyclic Amplitude		Period (min)	No. of Cycles
		Amplitude (mm)	Strain (%)		
1	100	0.5	≈ 0.7	14	10
2					15
3					20
4					110

Figure 4 presents the normalized stress plots and stress-strain relationships obtained from the additional tests. As the applied cyclic strain amplitude for these four tests has reduced by half to 0.7%, the number of load cycles required to reach the same mean effective stress state as previous tests with strain amplitude of 1.4% has increased proportionally. However, as Figure 4 shows, the post-cyclic effective stress paths of these four tests can still be categorized under the three normalized mean effective stress regimes previously discussed. The boundaries of these three regimes remain the same despite the

increase in number of load cycles and reduction in applied cyclic strain amplitude. This implies that the form of the effective stress paths of Singapore Upper Marine Clay under post-cyclic monotonic loading is dependent primarily on the mean effective stress state at the end of the cyclic loading phase.

4 CONCLUSIONS

The effective stress paths of Singapore Upper Marine Clay under post-cyclic monotonic loading takes on three different forms depending on the mean effective stress state of the specimen at the end of the cyclic loading phase. Although it is commonly accepted that the undrained post-cyclic effective stress path of a normally consolidated clay is similar to the effective stress path of an overconsolidated clay (Matsui and Abe 1981, Hyde and Ward 1985, Yasuhara et al. 1992), this study shows that this condition holds only when the normalized mean effective stress state of the clay specimen at the start of

post-cyclic monotonic loading falls below 0.5. When the normalized mean effective stress state of the clay specimen at the start of post-cyclic monotonic loading is greater than 0.6, the effective stress path of the specimen still follows that of lightly over-consolidated and normally consolidated clays. Within each of these normalized mean effective stress regimes, the post-cyclic clay behavior is governed by the normalized mean effective stress after cyclic loading and independent of the effective consolidation pressure, the cyclic strain amplitude and number of cycles applied during cyclic loading.

Furthermore, stress reversal points observed during cyclic loading phase becomes evident when mean effective stress state of the clay specimen at the start of post-cyclic monotonic loading falls below 0.5. Thus, the occurrence of stress reversal during cyclic loading is indicative of dilative behavior and post-cyclic monotonic loading in this regime exhibits effective stress path of an overconsolidated clay.

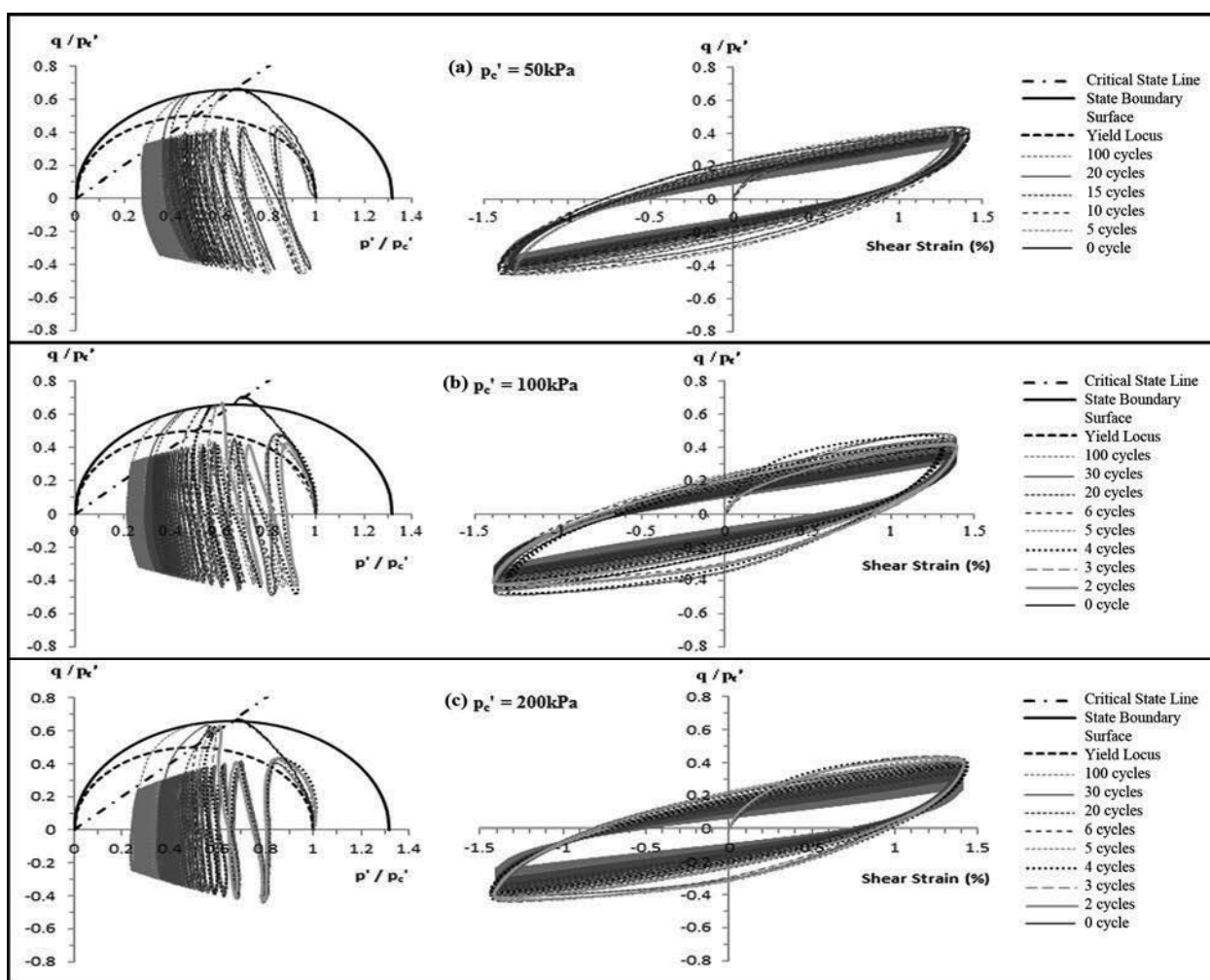


Figure 1. Effective Stress Paths and Stress-Strain Relationships for (a) $p_c' = 50\text{kPa}$, (b) $p_c' = 100\text{kPa}$, and (c) $p_c' = 200\text{kPa}$.

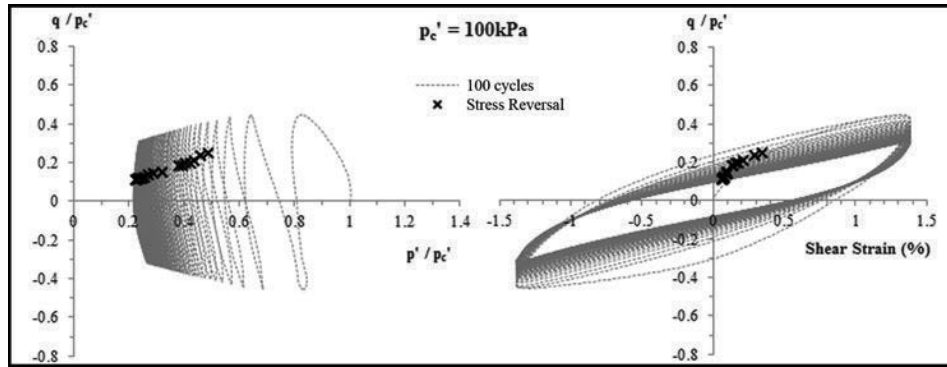


Figure 2. Stress Reversal Points.

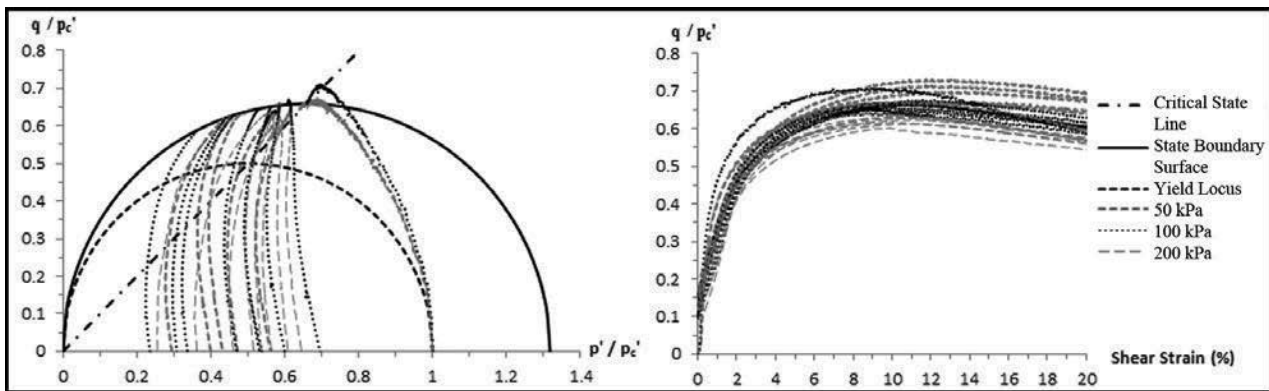


Figure 3. Post-cyclic Effective Stress Paths and Stress-Strain Relationships.

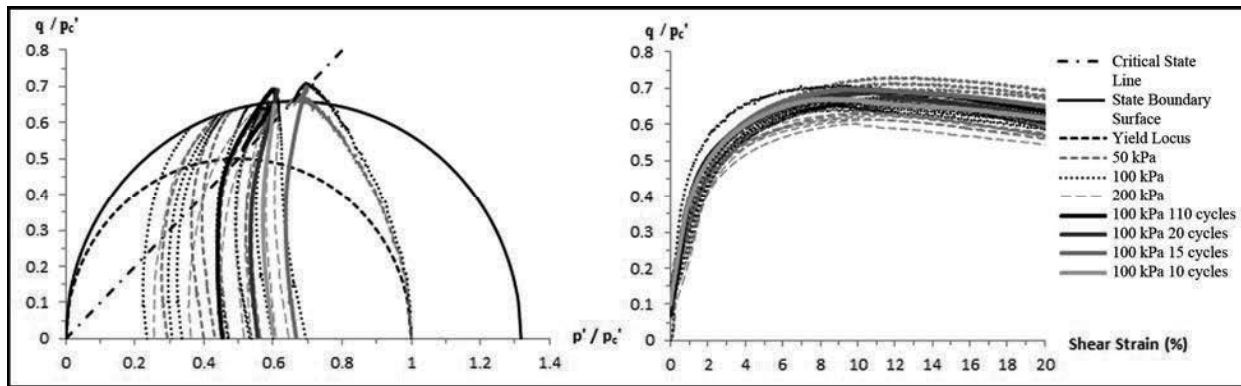


Figure 4. Post-cyclic Effective Stress Paths and Stress-Strain Relationships for Post-Cyclic Tests at 0.7% Cyclic Amplitude.

5 ACKNOWLEDGEMENTS

The authors are grateful to National University of Singapore for the provision of laboratory facilities, without which the research will not be possible. In particular, the main author will like to thank National University of Singapore for the research opportunity given through the award of research scholarship.

6 REFERENCES

Diaz-Rodriguez J.A., Moreno P. and Salinas G. 2000. Undrained shear behavior of Mexico City sediments during and after cyclic loading. Proc. 12th World Conference on Earthquake Engineering, 1652-1660.

Ho J.H., Kho Y., Goh S.H. and Lee F.H. 2012. Cyclic triaxial testing of soft clays. Proc. 25th KCCNN Symposium on Civil Engineering, 347-350.

Hyde A.F.L. and Ward S.J. 1985. A pore pressure and stability model for a silty clay under repeated loading. *Géotechnique* 35 (2), 113-125.

Tan S.L. 1983. Geotechnical properties and laboratory testing of soft soils in Singapore. Proc. 1st International Seminar on Construction Problems in Soft Soils, 1-47.

Thiers G.R. and Seed H.B. 1969. Strength and stress-strain characteristics of clays subjected to seismic loading conditions. Proc. ASTM STP 450, 3-56.

Wood, D.M. 1982. Laboratory investigations of the behaviour of soils under cyclic loading: a review. In: Soil mechanics – Transient and cyclic Loads, eds. Pande, G.N. and Zienkiewicz, O.C. John Wiley & Sons Ltd, Chichester.

Yasuhara K., Hirao K. and Hyde A.F.L. 1992. Effects of cyclic loading on undrained strength and compressibility of clay. *Soils and Foundations* 32 (1), 100-116.